Taylor & Francis
Taylor & Francis Group

RESEARCH ARTICLE

OPEN ACCESS   Check for updates

Vitamin D/vitamin D receptor/Atg16L1 axis maintains podocyte autophagy and survival in diabetic kidney disease

Lang Shi[a,b], Chao Xiao[b,c], Yafei Zhang[b], Yao Xia[b], Hongchu Zha[b], Jiefu Zhu[a] and Zhixia Song[b]

[a]Department of Nephrology, Renmin Hospital of Wuhan University, Wuhan, Hubei Province, China; [b]Department of Nephrology, The First Clinical Medical College of Three Gorges University, Center People's Hospital of Yichang, Yichang, Hubei, China; [c]Department of Nephrology, First Affiliated Hospital of Gannan Medical University, Ganzhou, Jiangxi, China

ABSTRACT

Objective: To investigate the effect of vitamin D/vitamin D receptor (VDR)/Atg16L1 signaling on podocyte autophagy and survival in diabetic nephropathy.

Methods: Diabetic rat models were induced by intraperitoneal injection of streptozotocin (STZ) (60 mg/kg) and treated with and without gavage of 0.1 μg/kg/d active vitamin D3 (aVitD3; 1,25-OH vitamin D3) and kidney tissues assessed by histopathology and immunohistochemistry. The murine podocyte cell line MPC-5 was cultured under hyperglycemic conditions in the absence or presence of 100 nmol/L calcitriol to investigate podocyte injury and autophagy. Cell survival rates were analyzed using Cell Counting Kit-8 (CCK-8) assays and the numbers of autophagosomes were determined after transduction with the mRFP-GFP-LC3 autophagy reporter construct. The expression of autophagy-related proteins (LC3-II, beclin-1, Atg16L1) and podocyte-related proteins (nephrin, podocin, synaptopodin, and desmin) was determined by Western blotting.

Results: VDR expression and autophagy were decreased in diabetic nephropathy. Calcitriol treatment repressed renal injury in rat diabetic kidneys and reduced high glucose-induced damage to cultured podocytes. Mechanistically, Atg16L1 was identified as a functional target of VDR, and siRNA-mediated knockdown of VDR and Atg16L1 blocked the protective effects of aVitD3 against podocyte damage.

Conclusion: Autophagy protects podocytes from damage in DN and is modulated by VitD3/VDR signaling and downstream regulation of Atg16L1 expression.

1. Introduction

Diabetic nephropathy (DN) is a severe complication of diabetes mellitus (DM) and represents one of the major complications associated with the morbidity and mortality of patients. DN is associated with about 40% of DM cases and almost 25% of these patients eventually develop uremia [1]. An abundance of recent studies has indicated that podocyte loss is the key process involved in DN development [2–4]. Previously we demonstrated that abnormal podocyte phenotypes together with related molecular expression changes provided hints of early DN pathogenesis [5]. Moreover, it has recently been disclosed that decreased autophagic activity plays a critical role in podocyte injury in DN [6].

Podocytes are highly differentiated epithelial cells that normally exhibit high levels of autophagy. Autophagy fulfills an essential housekeeping role by removing aggregated proteins and clearing damaged organelles. Consequently, autophagy is essential for preserving cellular homeostasis, for example, to resolve the effects of intracellular stress which leads to the accumulation of damaged proteins and organelles. Notably, there is increasing evidence showing that autophagy helps podocytes resist cellular damage to maintain their structural and functional integrity [7]. Consequently, the role of autophagy in DN has been explored in some detail. For instance, Xu et al. reported that glucose-induced podocyte dysfunction was related to a decline in autophagy [8]. Notably, in the context of a mouse model of DM induced by a high-fat diet, the depletion of autophagy-related genes causes podocyte death through apoptosis, causing heavy proteinuria [6]. Together these studies suggest that maintaining autophagy in podocytes is essential to preventing DN,

leading to the search for treatment interventions that could promote or maintain autophagy in podocytes.

Besides their essential role in calcium and phosphate metabolism, vitamin D3 and its receptor (vitamin D receptor, VDR) have been shown to contribute to renal protection [9]. For example, a recent clinical trial found that deficiency of 25-hydroxy vitamin D was an independent risk factor to predict the outcome of type 2 diabetes mellitus patients [10]. Furthermore, in animal models of type 1 and type 2 diabetes, the administration of vitamin D significantly reduces proteinuria as well as podocyte injury and loss [10–12]. Our previous work indicated that activated VitD3 (aVitD3) dramatically decreased proteinuria, glomerular hypertrophy and mesangial matrix deposition in a rat model of DN, with up-regulation of nephrin and podocin and decreases in the expression of podocyte injury markers. The structural stability of the podocytes is maintained by aVitD3, which rests with regulation VDR [5,13]. However, the precise mechanism(s) of renal protection offered by aVitD3 has not been fully elucidated. Nevertheless, in the context of DN, Wang et al. reported that VDR activation promoted autophagic flux *via* upregulation of Atg3 [14]. Whereas Li et al. showed that aVitD3 restored defective autophagy by stimulating CAMKK2 activation and AMPK phosphorylation [15]. Taken together these studies propose a vital function for aVitD3 in maintaining autophagy. The protein encoded by the Atg16L1 gene forms a complex with the autophagy-related proteins Atg5 and Atg12, to form part of the autophagy complex. Atg16L1 is functionally important for the formation and subcellular localization of autophagosomes and is involved in the lipidation and conversion of LC3-I to its membrane binding form LC3-II [16–18]. Therefore, we speculated that aVitD3 alleviated podocyte damage in DN through upregulation of VDR-Atg16L1 signaling. Hence, VDR-Atg16L1 could represent an underlying mechanism involved in the protection of DN by aVitD3.

2. Materials & methods

2.1. Clinical samples

Renal biopsies exhibiting diabetic nephropathy were collected from the First Clinical Medical College of Three Gorges University. Exclusion criteria included the coexistence of other primary and secondary kidney diseases, such as membranous nephropathy or lupus nephropathy. Non-tumor kidney tissue from surgical specimens of patients who had renal carcinoma was used as normal controls. All patients provided written informed consent. Demographic, laboratory, and renal pathological data were recorded. Renal biopsy specimens were collected for measuring the numbers of autophagosomes under transmission electron microscopy and VDR expression using immunohistochemistry [19]. We adopted the double-blind evaluation method for analysis. Renal biopsies tissue was homogenized in RIPA buffer and centrifuged at 12,000 rpm for 30 min. The supernatant (SN) was collected for use in ELISA analysis. VDR levels were determined using Human VDR ELISA Kit (Jonln, Shang Hai, JL13098-96T).

2.2. Rat model of diabetes

Specific pathogen-free Sprague-Dawley (SD) male rats (180–200 g, 6 weeks old) were provided by the Experimental Animal Center of the Three Gorges University School of Medicine. The diabetes model based on the administration of streptozotocin (STZ) was established as previously described [19].

2.3. Histopathology

Periodic Acid-Schiff (PAS) staining was performed according to the manufacturer's instructions (Servicebio, Wuhan, China). The extent of renal injury was estimated by the morphometric assessment of the mesangial matrix expansion and the enlargement of the glomeruli. A point-counting method was used to quantify mesangial matrix deposition. The staining was evaluated in 20 randomly selected glomeruli using a $40 \times$ objective. The score in each rat was expressed as the mean value of all the scores obtained.

2.4. Immunohistochemistry

The histological section of renal (3 μm) was used for immunohistochemical staining of VDR (catalog no. sc-13133, Santa Cruz, USA) and Beclin1 (catalog no. BN500-249, Novus, USA) proteins. After antigen retrieval with sodium citrate buffer, sections were incubated with a primary antibody, and then the specimen was incubated with a species-specific secondary antibody (Millipore, USA). Subsequently, the sections were visualized with diaminobenzidine (Maixin, China) and the nuclei were counterstained with hematoxylin. The staining intensity was observed under a light microscope and assessed by IHC Profiler in Image J software (Media Controbernetics Inc, Rockville, USA), and 20 consecutive non-repetitive fields of view were taken from the kidney of each rat.

2.5. Cell culture and treatment

Conditionally immortalized mouse podocytes (MPC-5) (kindly provided by Peter Mundel, Mount Sinai School of Medicine through Prof. Aihua Zhang at Nanjing Medical University, Nanjing, China) were induced to differentiate as previously described [19]. Briefly, the cells were cultured in a DMEM-F12 medium containing 10% fetal bovine serum and mouse recombinant IFN-γ (10 U/mL) at 33 °C, 5% $CO2$. To induce differentiation, podocytes were cultured in a medium without IFN-γ for 10–14 days. Fully differentiated cells at 80% confluence were used for the subsequent experiments. For euglycemic or hyperglycemic conditions, the cells were cultured in a medium containing 5.5 mmol/L or 30 mmol/L glucose, and 24.5 mmol/L mannitol, respectively, for 24 h.

2.6. Western blot

Cell and tissue lysates were prepared using RIPA buffer and equal protein amounts resolved on 10% SDS-PAGE gels before transfer to PVDF membranes. The membranes were then blocked and incubated with primary antibodies against nephrin (catalog no. Ab216341, Abcam, UK), beclin1 (catalog no. NB500-249 Novus, USA), podocin (catalog no. Ab181143 Abcam, UK), synaptopodin (catalog no. sc-515842 Santa Cruz, USA), desmin (catalog no. Ab8592 Abcam, UK), LC3 (catalog no. NB100-2220 Novus, USA) and Atg16L1 (catalog no. A1871; ABdonal) overnight. Protein bands levels were detected and analyzed using Image-Pro plus software with β-actin used as the internal reference.

2.7. Cell viability detection

Cell viability was determined using the Cell Counting Kit-8 (CCK-8) according to the manufacturer's instructions. Briefly, MPC-5 cells in the logarithmic growth stage were seeded into a 96-well plate at a density of 2×10^3/well and allowed to attach for 12 h. After the addition of CCK-8 reagent for 24 h, the mean optical density (OD) was determined for each treatment group to calculate cell viability as a percentage: percentage of cell viability $=$ ODtreatment/ODcontrol$\times$ 100%.

2.8. Adenovirus transduction

MPC-5 cells were seeded onto glass coverslips in 24 well plates at a density of 1×10^5/well before the addition of recombinant adenovirus encoding the mRFP-GFP-LC3 protein (multiplicity of infection (MOI) was 40) (Hanbio, Shanghai, China). The cells were incubated with an adenovirus mixture (250 μL/well) for 6 h, and then the media was exchanged for a fresh culture medium and the cells were incubated for another 72 h. Thereafter, the cells were cultured in the presence of various treatments for 24 h, followed by staining with DAPI (2μl/mL) for 5 min. After washing the cells 3 times with PBS, the cells were fixed and the coverslips mounted onto glass slides before imaging with a confocal microscope. For quantitative analysis, approximately 100 transfected cells from 10 to 20 random fields ($\times$630) were analyzed in each condition. The numbers of GFP-LC3 puncta per cell and RFP-LC3 puncta per cell were counted separately using ImageJ. The number of autophagosomes was indicated by GFP dots and the number of autolysosomes was obtained by subtracting GFP dots from RFP dots.

2.9. Cell transfection

For euglycemic or hyperglycemic conditions, the cells were cultured in a medium containing 5.5 mmol/L or 30 mmol/L glucose, respectively, for 24 h, then transiently transfected with siRNA VDR and siRNA atg16L1 using X-treme GENE transfection reagent (Roche, USA) according to the manufacturer's instructions. siRNA VDR GTCTTTCACCATGGATGATAT, siRNA VDR scramble ACAG CUACAACUAUCAUCACU, siRNA Atg16L1 TCTGGATTCTA TCACTAATAT, siRNA Atg16L1 scramble CACAACCUACC GACACUCACG. All sequences were synthesized by Sangon Biotech Co., Ltd (Shanghai, China).

2.10. Statistical analysis

All statistical analyses were performed by GraphPad Prism 8.0 software (CA, USA). Two-tailed Student's t-test and Mann-Whitney U test were used for two-group comparisons with normal distribution and non-normal distribution, respectively. Kruskal-Wallis test and one-way ANOVA with Tukey's multiple comparison test were used for multi-group comparisons with the non-parametric and parametric tests, respectively. P values less than 0.05 were considered to represent statistically significant differences.

3. Results

3.1. VDR expression and autophagy are decreased in diabetic nephropathy

An increasing body of evidence suggests that autophagy and VDR dysregulation are closely tied to diabetic kidney disease. To explore this concept, we examined the expression of the autophagy-related marker,
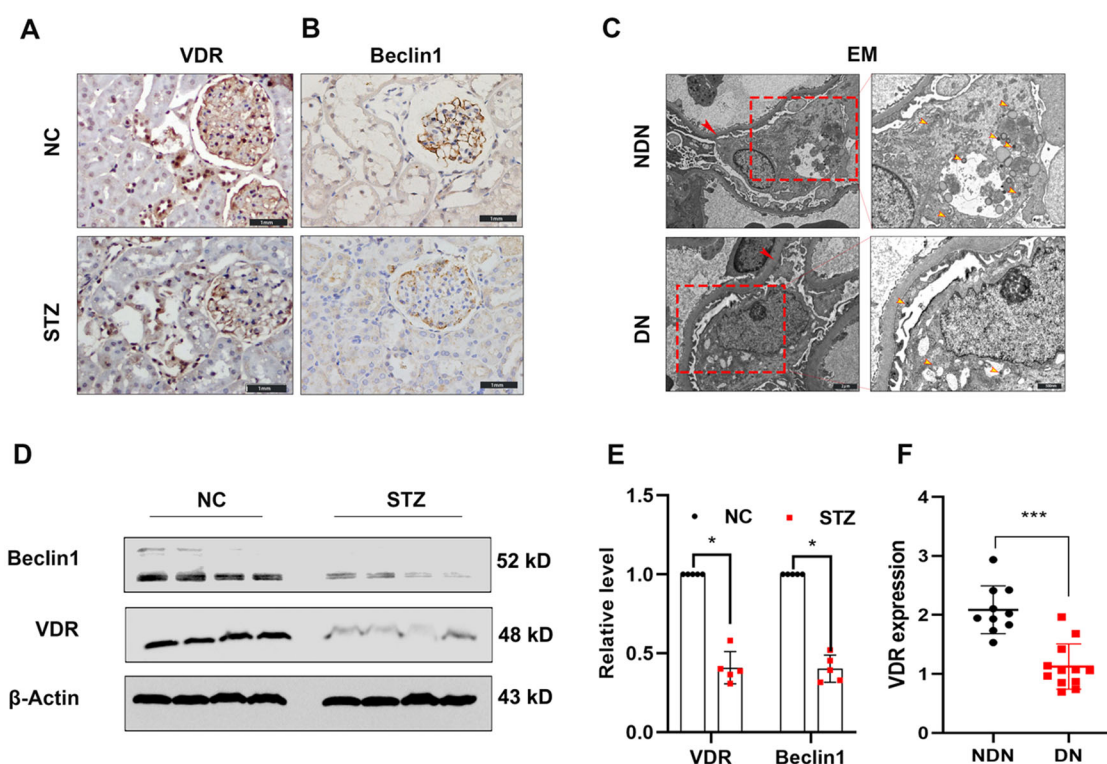
Figure 1. The expression of VDR protein and autophagosomes is down-regulated in diabetic kidneys. (A) The VDR level was detected by immunohistochemical staining ($\times 400$). (B) Representative pictures of anti-beclin1 immunohistochemical staining ($\times 400$). (C) Kidney biopsy specimens were from patients with diabetic nephropathy (DN) and non-tumor renal tissue from patients with kidney cancer. Representative ultrastructural imagines showing the double-membraned vesicles (autophagosomes) in podocytes. Basement membrane (red arrows) and autophagosomes (yellow arrow). (D) Western blot analysis of VDR and Beclin1 in the renal cortex of rats from each group as indicated. (E) Relative expression of proteins levels. (F) The VDR levels in patients with diabetic nephropathy (DN) and non-tumor renal tissue from patients with kidney cancer were measured by ELISA. Data were presented as mean ± SD. ***$p < 0.001$.

beclin1 along with the expression of VDR in the kidneys of normal control (NC) and diabetic (streptozotocin-treated (STZ) rats. We found VDR was mainly expressed in glomerular podocytes and tubular epithelial cells, with staining significantly decreased in STZ-treatment rats. Consistent with this result, the parallel immunoblotting analysis showed that the levels of VDR were comparatively reduced in STZ-treatment rats (shown in Figures 1A and D). Moreover, the levels of beclin1 expression were also significantly decreased in the kidneys of STZ-treatment rats compared with the vehicle control groups (shown in Figures 1B and D). To verify these findings in the clinical setting, we collected kidney biopsy specimens from 12 patients with diabetic nephropathy and compared these with normal (para-cancer) kidney tissues collected from surgical resection of 10 patients with renal cancer. In electron microscopy, autophagosomes are identified as double-membrane structures with immuno-gold labeling LC3 [20]. In this study, the characterized double-membrane vesicles are considered autophagosomes without specific immuno-gold labeling. Expression of VDR and autophagosomes

in podocytes was reduced in diabetic kidneys compared to normal kidney tissues detected by enzyme-linked immunosorbent assay (Figure 1F) and electron microscopy (Figure 1C) respectively. These clinical findings and *in vivo* studies indicated both VDR expression and autophagy defects of podocytes in diabetic nephropathy.

3.2. Active vitamin D3 represses renal injury in STZ-induced diabetic rat kidneys and HG-treated podocyte damage

We then turned to examine the effects of an aVitD3 intervention in the STZ-induced rat model of diabetes. Histological examination of the diabetic rat kidney showed a significant deposition of periodic acid Schiff (PAS) staining material in the interstitium. Positive PAS staining indicates an expanded mesangial matrix in the glomerular area, which was significantly attenuated by aVitD3 treatment (Figure 2A). These results demonstrate that aVitD3 interventions have the potential to limit HG-induced podocyte damage *in vitro* and ameliorate
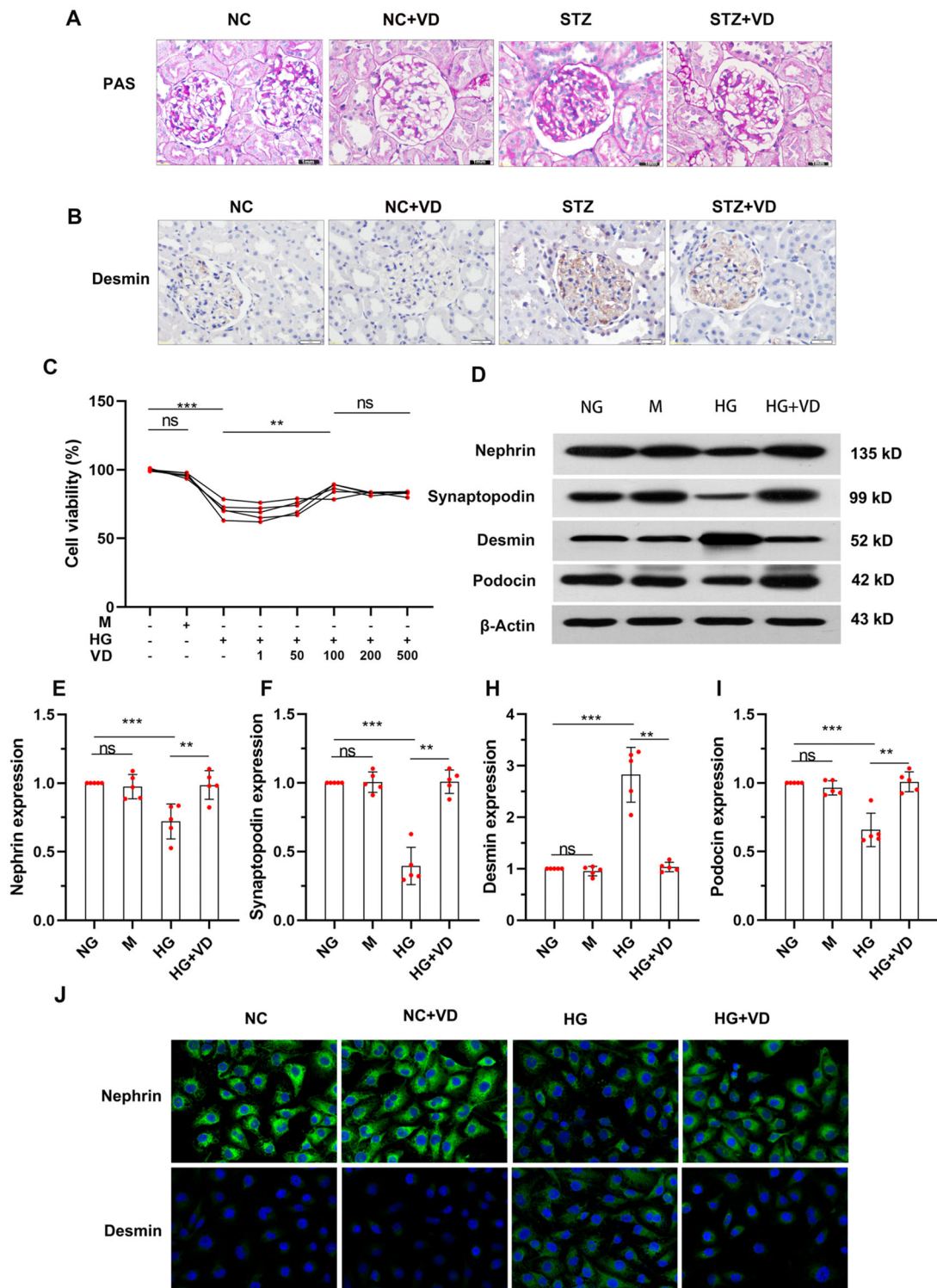
Figure 2. Renal failure in STZ-induced diabetic rats and *in vitro* MPC-5 injury stimulated with high-glucose was alleviated by aVitD3. (A) PAS staining of kidney sections. SD male rats were intraperitoneally injected with 60 mg/kg streptozotocin. After 3 days, the rats with STZ treatment were garaged with 0.1 μg/kg/d calcitriol or vehicle solution daily for consecutive 18 weeks. Kidney tissues were collected for histology. (B) Representative images of immunohistochemical staining for desmin in the renal cortex at 18th week (×400). (C) MPC-5 cells viability. After being administered with different doses of aVitD3 (1–500 nmol/L) for 24 h, the MPC-5 cells viability was determined by CCK-8 assay. MPC-5 were cultured for 24h in a medium with 30 mM glucose or 5.5 mM glucose in the absence or presence of 100 nmol/L aVitD3. (D) Representative western blot images of Nephrin, Podocin, Synaptopodin and Desmin expression. (E–I) Relative expression of proteins levels. Band densities were measured by the ImageJ program. The ratio of protein/actin density was calculated and normalized with the sham controls. Data were presented as mean ± SD. $n = 4$. $**p < 0.01$. $***p < 0.001$. (J) Immunofluorescence staining of nephrin and desmin in a medium containing NG, VD, HG and HG plus aVitD3 for the indicated periods (×400).

renal injury in diabetic kidneys *in vivo*. Next, we explored the effects of aVitD3 on the levels of injury in cultured MPC-5 podocytes induced by high-glucose (HG, 30 mmol/L) treatment. In order to exclude the effect of high sugar as the hypertonic solution on osmotic pressure, mannitol (M, 24.5 mmol/L) treatments were used as an osmotic control in these experiments with cell survival rates determined using CCK-8 assays. As expected, there were significant differences in cell survival rates between the normal glucose (NG, 5.5 mmol/L) and mannitol (M) groups, but cell survival levels significantly decreased after HG treatment. Instructively, the addition of aVitD3 enhanced the viability of MPC-5 cells exposed to HG with the effects achieving a plateau at 100 nmol/L of aVitD3 (shown in Figure 2C, $p < 0.01$). Thus, 100 nmol/L aVitD3 treatments were used in subsequent experiments. Western blotting analysis showed that the protein expressions of nephrin, podocin and synaptopodin were decreased, while desmin was up-regulated in high glucose compared with the normal glucose group (shown in Figure 2D–I). This suggests that high glucose can cause podocyte damage, consistent to the previous studies [5,19], and these podocyte injuries can be reversed by aVitD3 treatment (Figure 2D–I). Immunofluorescence results confirm that aVitD3 preserved nephrin and suppressed desmin under high glucose (Figure 2J).

3.3. The aVitD3/VDR pathway positively regulates autophagy in podocytes

Next, we explored the effect of the VitD3 on autophagy *in vivo and vitro*. Glomerular Beclin1 level was suppressed in STZ-treated mice, which was preserved by aVitD3 treatment (Figure 3A). MPC-5 cells were treated with high glucose and the changes in autophagosome numbers were assessed through the appearance of dual RFP-GFP (yellow) fluorescence puncta after transduction with LC3-RFP-GFP. Compared to the HG group that had fewer puncta of GFP-LC3 and RFP-LC3 puncta indicating a low basal level of autophagy, aVitD3 and rapamycin significantly induced the formation of autophagosomes as well as the maturation to autolysosomes in podocytes. As shown in Figure 3B, autophagosomes were decreased under high glucose conditions and were further decreased after treatment with the autophagy inhibitor 3-methyladenine (3-MA) which inhibits the fusion of autophagosomes with lysosomes and prevents lysosomal protein degradation. These results further indicate that high glucose impairs autophagic flux. Conversely, treatment with aVitD3 and rapamycin (Rap), an autophagy agonist, led to increased autophagosomes, as shown by the increased yellow puncta compared with the HG group, indicating increases in autophagic flux. Moreover, the expression of LC3-II was increased when cells were treated with aVitD3 under high glucose conditions (shown in Figures 3C and D). Lastly, we used siRNA transfection to knock down VDR to investigate the role of VDR in autophagy regulation. Notably, LC3 expression decreased significantly when VDR was silenced, indicating that active vitamin D3 upregulates autophagy through VDRs (shown in Figures 3C and D).

3.4. VDR siRNA blocks the protective effects of aVitD3 on podocytes

Recent studies suggest that VDR is involved in the regulation of autophagic flux and VDR deficiency might contribute to podocyte injury in DN [14,15]. To verify this mechanism, we assessed the survival rate of MPC-5 cells under HG conditions after depleting VDR expression with siRNA. Notably, compared to the HG + VD group, the survival rate of MPC-5 cells in the HG + VD + VDR siRNA group was significantly decreased (shown in Figure 4B, $p < 0.01$). In addition, the HG + VD + VDR siRNA group showed lower protein expression of nephrin, podocin and synaptopodin, and higher expression of desmin compared to the HG + VD group（shown in Figure 4C–H, $p < 0.05$). These results suggested that VDR activation represents a key mechanism underlying vitamin D3 protection of podocytes under high glucose conditions.

3.5. Atg16L1 is a target gene of VDR in podocytes

VDR is fundamentally a transcription factor that directly regulates downstream gene transcription by binding with target gene promoters in the nucleus. Some of the direct target genes of VDR are autophagy regulators, for example, VDR expression in intestinal epithelial cells drives the expression of the Atg16L1 gene to delay the progression of inflammatory bowel disease [21]. We consequently determined if the Atg16L1 gene was regulated by VDR in podocytes. Using the JASPAR database (http://jaspar.genereg.net), bioinformatics analysis predicted a VDR binding site in the gene promoter of Atg16L1 (shown in Figure 5A). Analysis of Atg16L1 levels by Western blotting showed that the HG + VD + VDR siRNA group had lower levels of Atg16L1 protein compared to the HG + VD group. The results indicated that HG treatment reduced the protein expression of Atg16L1 *via* the VDR (shown in Figures 5B and C, $p < 0.05$).
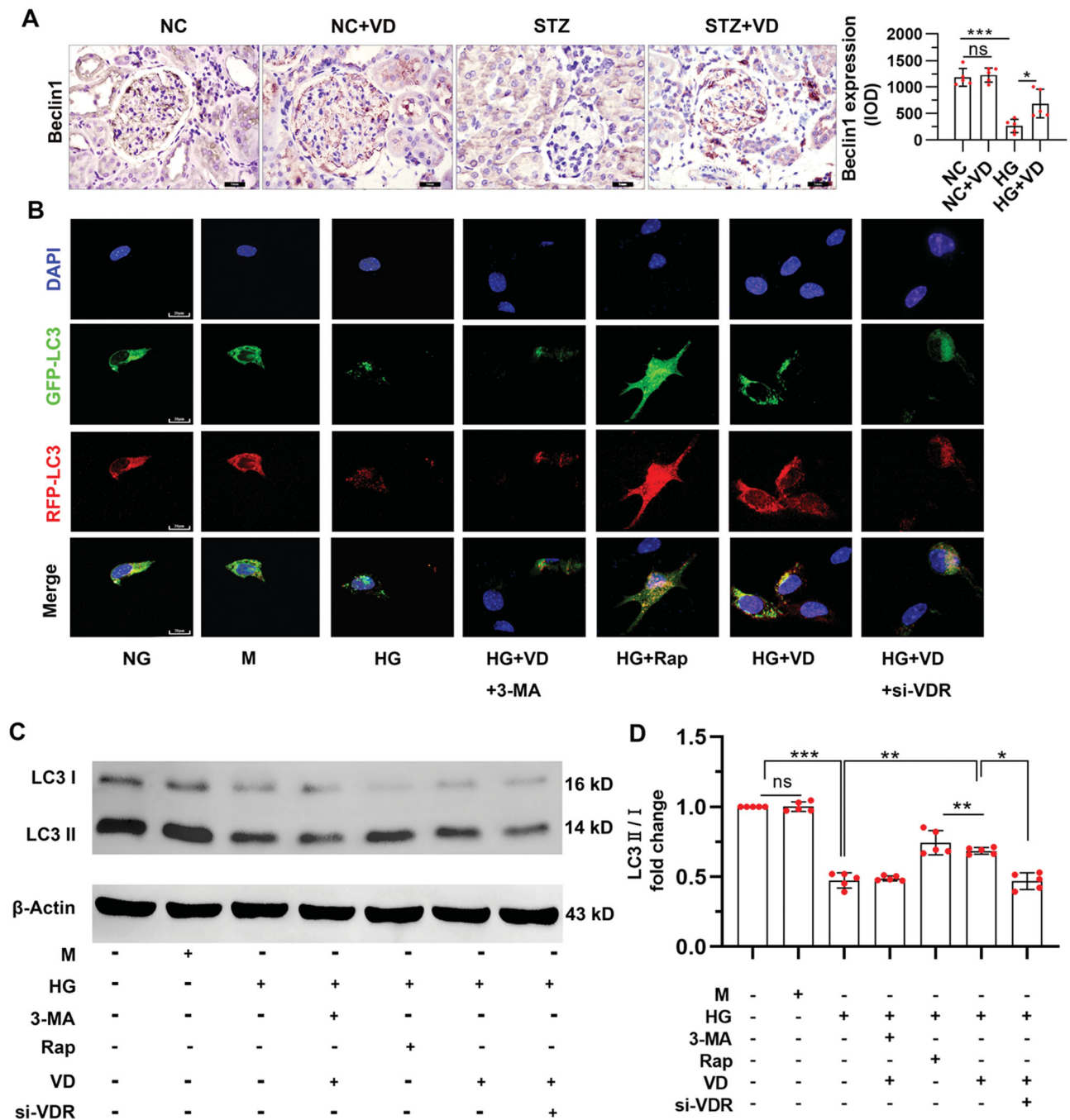
Figure 3. Effect of aVitD3 treatment on autophagy in vivo and *vitro*. (A) Representative images and quantitative analysis of immunohistochemical staining for beclin1 (×400). SD male rats were intraperitoneally injected with 60 mg/kg streptozotocin. After 3 days, the rats with STZ treatment were garaged with 0.1μg/kg/d calcitriol or vehicle solution daily for consecutive 18 weeks. Kidney tissues were collected for immunohistochemical staining (B) Immunofluorescence analysis of LC3 puncta in MPC-5 cells of each group as indicated. Representative images of GFP-LC3 and RFP-LC3 fluorescence staining (×630). Scale bar: 20 μm. (C) Western blot analysis of LC3 in MPC-5 cells from each group as indicated. (D) Relative expression of proteins levels. Band densities were measured by the ImageJ program. The ratio of protein/actin density was calculated and normalized with the sham controls. Data were presented as mean ± SD. n = 5. *$p < 0.05$, **$p < 0.01$, ***$p < 0.01$.

3.6. Atg16L1 regulates the protective effects of aVitD3 on podocytes

We then determined if Atg16L1 expression was required to elicit the protective effects of aVitD3 on MPC-5 cell survival under HG conditions. We assessed the survival rate of MPC-5 cells under HG conditions after depleting Atg16L1 expression with siRNA (shown in Figure 6A). Notably, compared to the HG + VD group, the survival
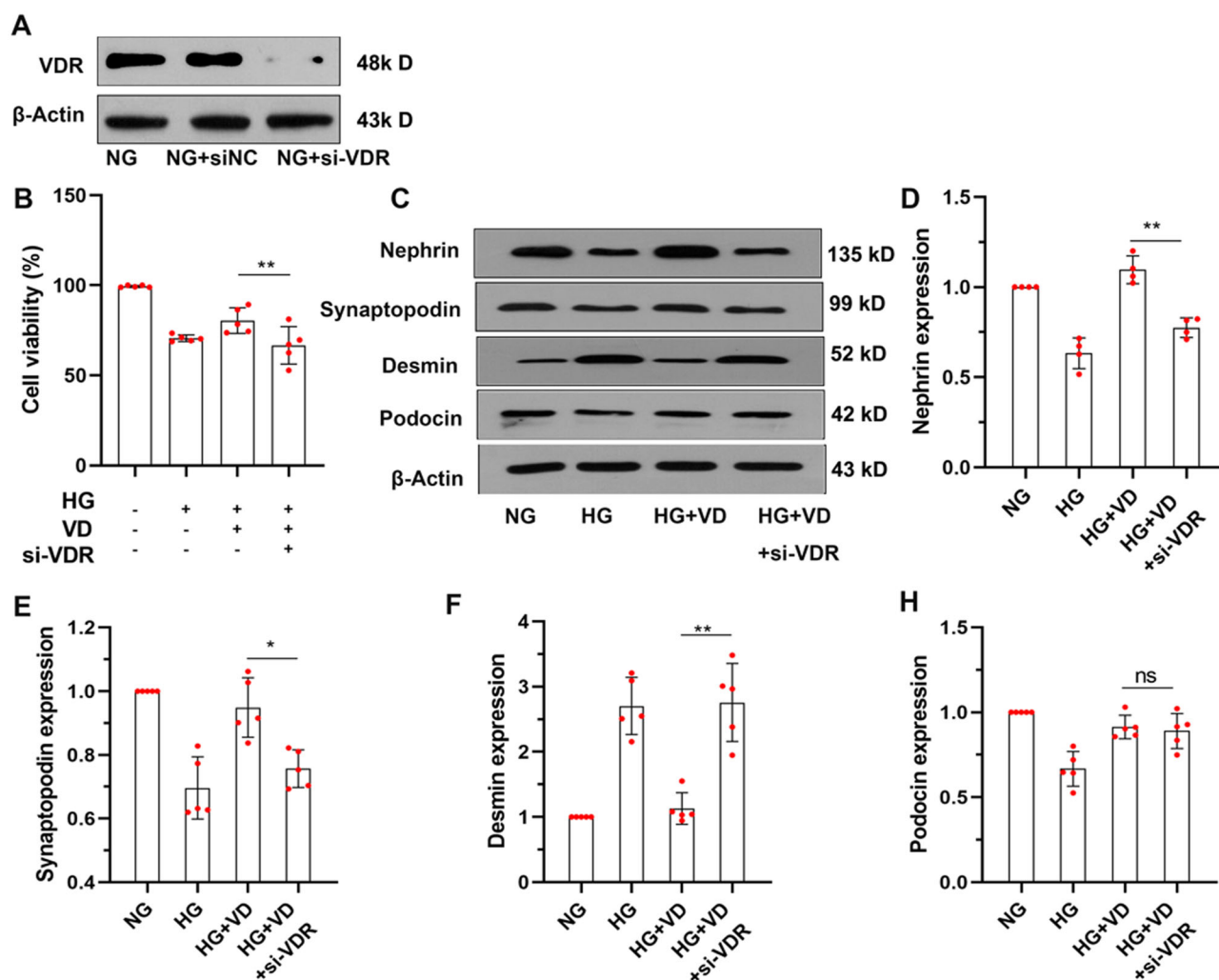
Figure 4. VDR siRNA knocked down VDR reduced the protective effect of aVitD3 on MPC-5 injury Induced by high glucose. MPC-5 cells were transfected with VDR siRNA (si-VDR) or normal control siRNA (si-NC) and subjected to the indicated treatment. (A) Representative image of VDR immunoblot. (B) The MPC-5 cells' viability was determined by the CCK-8 assay. (C) Nephrin, Podocin, Synaptopodin and Desmin expression. Representative images from Western blot results. (D–H) Relative expression of proteins levels. Band densities were measured by the ImageJ program. The ratio of protein/actin density was calculated and normalized with the sham controls. Data were presented as mean ± SD. $n = 5$. $**p < 0.01$.

rate of MPC-5 cells in the HG + VD + Atg16L1 siRNA group was significantly decreased (shown in Figure 6B, $p < 0.01$). After silencing Atg16L1, we observed that the protein levels of nephrin, podocin and synaptopodin were all lower in the HG + VD + Atg16L1 siRNA group than in the HG + VD group (shown in Figure 6C–I). In contrast, desmin protein levels were higher in the HG + VD + Atg16L1 siRNA compared to the HG + VD group (shown in Figure 6C–I). Together these results indicated that Atg16L1 silencing suppressed the protective effects of aVitD3 on MPC-5 viability, integrity and autophagy under high glucose conditions.

4. Discussion

Vitamin D3 is a multi-functional signaling molecule best known for regulating calcium and phosphate homeostasis to maintain healthy bones. Our previous research showed that treating podocytes with aVitD3 increases their expression of nephrin and podocin, but decreased the expression of the podocyte injury marker, desmin [19]. In this study, we found high glucose-induced downregulation of the autophagic regulator Atg16L1, while the intervention with aVitD3 significantly reversed Atg16L1 downregulation. The protective effects of aVitD3 disappeared when Atg16L1 was silenced. This suggests that aVitD3 upregulates autophagy to reduce high glucose-induced podocellular injury, possibly through the VDR-Atg16L1 signaling axis (Figure 7).

The vitamin D receptor (VDR) is a nuclear, ligand-dependent transcription factor belonging to the superfamily of nuclear receptors that are complex with the hormone aVitD3 [22]. Interaction with aVitD3 induces
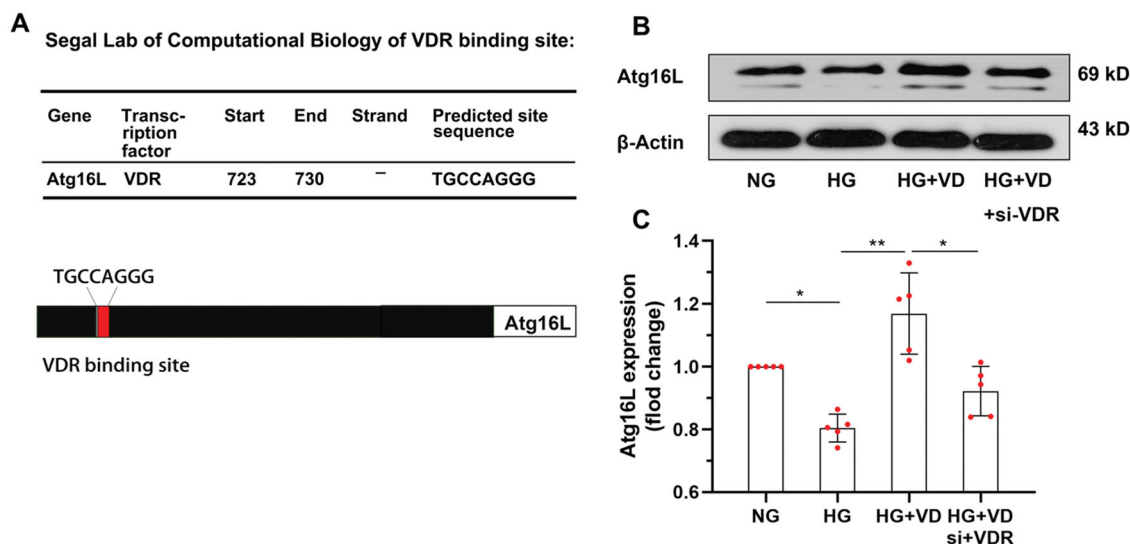
Figure 5. Atg16L1 was identified as VDR Target. (A) Predicted VDR binding site in Atg16L1 gene promoter. Pattern diagram of binding sites. (B) Western blot analysis of Atg16L1 in MPC-5 cells from each group as indicated. (C) The relative expression of Atg16L1 was normalized with the normal glucose control. $n = 5$. $*p < 0.05.**p < 0.01$.

the dimerization of VDR which then translocate to the nucleus to bind to vitamin D response elements (VDRE) occurring in more than 900 target genes, resulting in their up- or downregulation and eliciting regulation of a wide array of physiological functions [23,24]. Our study revealed that the expression of VDR and beclin1 were lower than in the kidneys of diabetic rats (shown in Figures 1 and 3A). Furthermore, we confirmed there were significant reductions in VDR activity and the numbers of autophagosomes in podocytes in diabetic kidneys compared to para-cancer normal kidney tissues (shown in Figure 1C and F).

Autophagy is a lysosome-dependent process that recycles damaged proteins and organelles, representing an essential process for maintaining normal cellular phenotype and functions [25]. However, when the pathological stress is too strong to bear, there might be autophagic disorder sabotaging cellular homeostasis and consequently leading to cell death [26]. Recent studies have highlighted the importance of autophagy in preventing podocyte injury in DN [19]. In the current study, we found high glucose exposure in murine podocytes altered several key proteins, including the downregulation of nephrin, podocin, synaptopodin and LC3, as well as up-regulation of desmin, together indicating that podocytes injury was accompanied by reductions in autophagy. Nevertheless, the addition of exogenous aVitD3, increased the expression of nephrin, podocin, synaptopodin and LC3 while the expression of desmin decreased. This suggested that aVitD3 provided protective effects against high glucose-induced podocyte injury by reversing autophagy deficiency (shown in Figures 2 and 4C). In the *in vivo* context, kidneys

showed a significantly better histological appearance after aVitD3 treatment (shown in Figures 2A and B). These results demonstrate that aVitD3 can prevent podocyte injury in DN through modulating autophagy.

Mechanistically, we established a role for the VDR in positively regulating the expression of the Atg16L1 gene in podocytes under high glucose conditions. The Atg16L1 protein is a core complex component essential for LC3 lipidation and autophagosome formation. Previous research has shown that intestinal epithelial VDR delays the progression of inflammatory bowel disease by regulating the expression of Atg16L1, sustaining the viability of Paneth cells and promoting microbial assemblage to maintain intestinal homeostasis [21]. In this study, we observed that high glucose-induced decreased Atg16L1 expression and autophagy in podocytes. However, the decreased expression of Atg16L1 could be reversed after intervention with aVitD3, but notably, the aVitD3 effects on Atg16L1 disappeared when VDR was silenced (shown in Figure 5B). VDRs are members of the ligand-regulated transcription factor and nuclear receptor superfamily, suggesting that VDR may be involved in the regulation of Atg16L1 gene transcription. Indeed, a VDR binding site was predicted in the promoter sequence of the Atg16L1 gene (TGAGTTTA) in the JASPAR database. Moreover, it has been shown that vitamin D3 treatment increased VDR and Atg16L1 protein expression, which activated autophagic responses [27]. We found that protective effects of aVitD3 disappeared when Atg16L1 was silenced, indicating that aVitD3/VDR protection against high glucose-induced podocyte damage occurs in an Atg16L1-dependent manner (shown in Figures 6C and D).
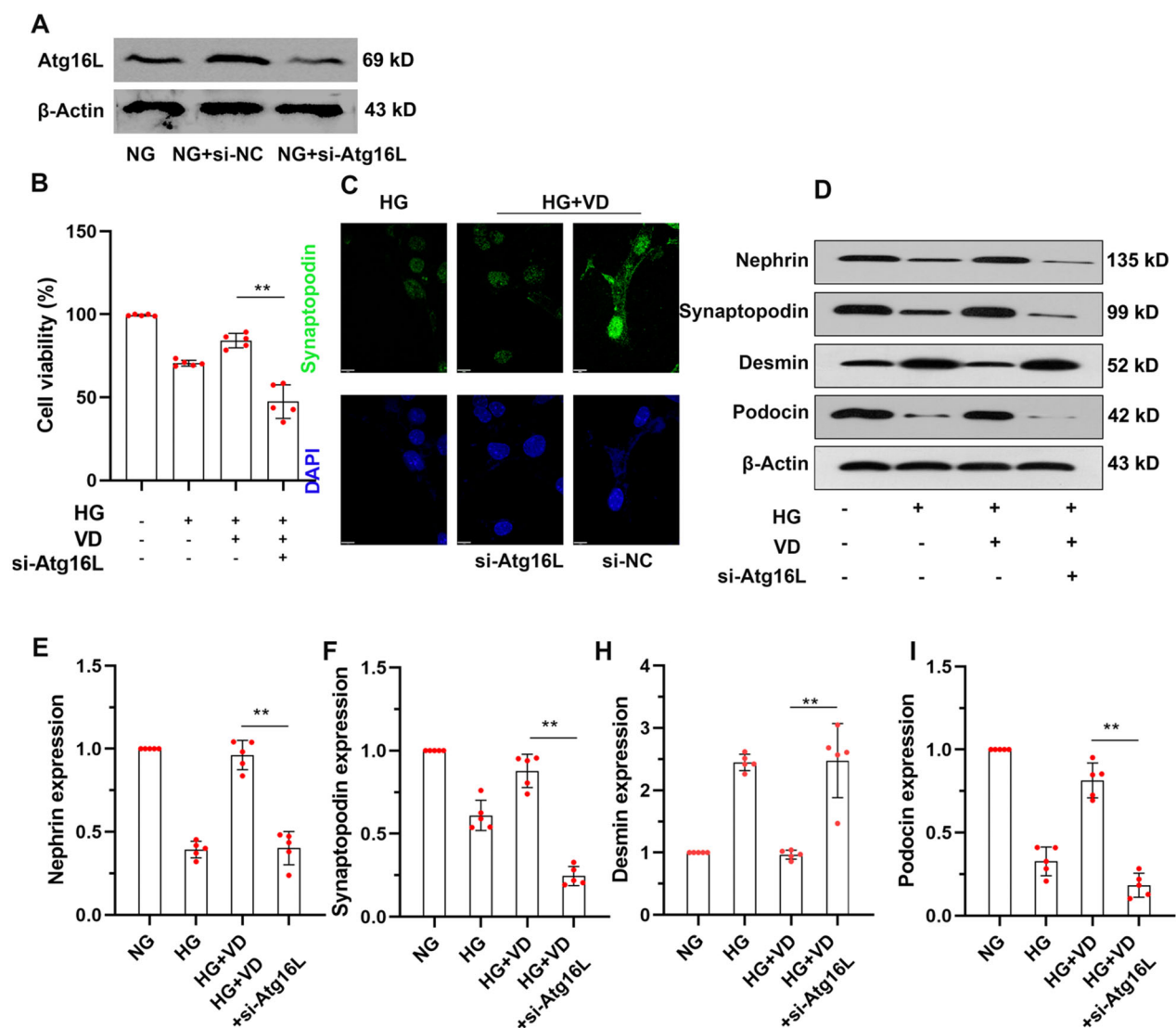
Figure 6. Atg16L1 siRNA Knocked Down Atg16L1 and reduced protective effect of aVitD3 on MPC-5 injury Induced by high-glucose. MPC-5 cells were transfected with Atg16L1 siRNA (si-Atg16L1) or normal control siRNA (si-NC) and subjected to the indicated treatment. (A) Representative image of Atg16L1 immunoblot. Proteins were extracted from the cells, and Atg16L expression was detected by Western blotting. (B) The cell viability analysis. (C) Immunofluorescence (IF) assays of Synaptopodin (green) and DAPI (blue) images of cultured MPC-5 under high-glucose conditions or treated with aVitD3, si-NC, si-Atg16L1 respectively. (D) Representative immunoblot images of Nephrin, Podocin, Synaptopodin and Desmin. (E–I) Relative expression of proteins levels. Band densities were measured by the ImageJ program. The ratio of protein/actin density was calculated and normalized with the sham controls. Data were presented as mean ± SD. $n = 5$. $**p < 0.01$.
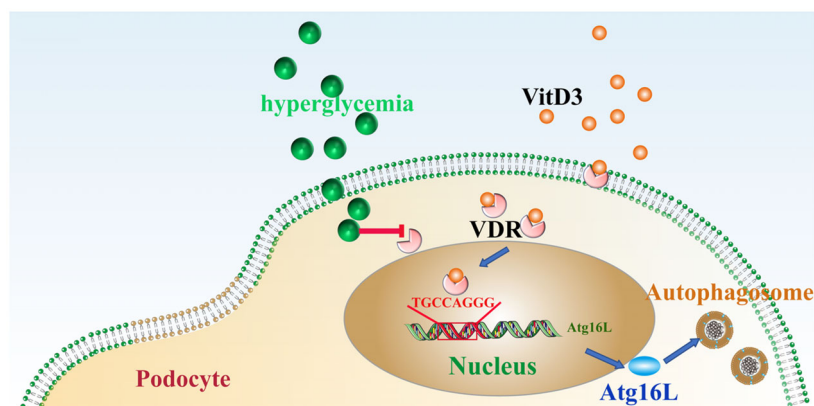

Figure 7. The working model of the VDR/Atg16L1 axis regulates autophagy activity in diabetic nephropathy.

In conclusion, this study demonstrated that VDR expression was impaired in the context of DN. We showed that the decreases in VDR expression under high glucose conditions mediated the downregulation of Atg16L1, resulting in autophagic deficiencies in podocytes. Notably, aVitD3 treatment alleviated podocyte injury through maintaining Atg16L expression and autophagic activity, thus preventing the progression of DN.

Conclusions

Active vitamin D3 regulates autophagy protects renal podocytes by VDR/Atg16L1 signaling axis.

Ethics statement

The trial was conducted in accordance with the Declaration of Helsinki. The study protocols were approved by the Human Subjects Committee of the First Clinical Medical College of Three Gorges University (HEC-KYJJ2019-053-01) and informed consent was taken from all the patients. All animal care and experimental programs are in the compliance with animal management regulations of the Ministry of Health of the People's Republic of China and approved by the Ethics Committee of the Three Gorges University (2017-0012).

Disclosure statement

The authors have no conflicts of interest to declare.

Funding

Author contributions

Zhixia Song and Jiefu Zhu contributed to the conception of the study; Lang Shi, Chao Xiao, Yafei Zhang, Yao Xia performed the experiment; Zhixia Song and Jiefu Zhu contributed significantly to analysis and manuscript preparation; Lang Shi performed the data analyses and wrote the manuscript; Chao Xiao, Yao Xia, Hongchu Zha helped perform the analysis with constructive discussions. Zhixia Song reviewed the manuscript.

Funding

Data availability statement

The authors are accountable for all aspects of the work in ensuring that questions related to the accuracy or integrity of any part of the work are appropriately investigated and resolved.

References

[1] Zhang L, Wang F, Wang L, et al. Prevalence of chronic kidney disease in China: a cross-sectional survey. Lancet. 2012;379(9818):815–822.

[2] Bonegio R, Susztak K. Notch signaling in diabetic nephropathy. Exp Cell Res. 2012;318(9):986–992.

[3] Li JJ, Kwak SJ, Jung DS, et al. Podocyte biology in diabetic nephropathy. Kidney Int Suppl. 2007;72(106): S36–S42.

[4] Stitt-Cavanagh E, MacLeod L, Kennedy C. The podocyte in diabetic kidney disease. ScientificWorldJournal. 2009;9:1127–1139.

[5] Song Z, Guo Y, Zhou M, et al. The PI3K/p-Akt signaling pathway participates in calcitriol ameliorating podocyte injury in DN rats. Metabolism. 2014;63(10): 1324–1333.

[6] Tagawa A, Yasuda M, Kume S, et al. Impaired podocyte autophagy exacerbates proteinuria in diabetic nephropathy. Diabetes. 2016;65(3):755–767.

[7] Hartleben B, Godel M, Meyer-Schwesinger C, et al. Autophagy influences glomerular disease susceptibility and maintains podocyte homeostasis in aging mice. J Clin Invest. 2010;120(4):1084–1096.

[8] Xu L, Fan Q, Wang X, et al. Ursolic acid improves podocyte injury caused by high glucose. Nephrol Dial Transplant. 2017;32(8):1285–1293.

[9] Holick MF. Vitamin D: a millenium perspective. J Cell Biochem. 2003;88(2):296–307.

[10] Cheng J, Zhang W, Zhang X, et al. Efficacy and safety of paricalcitol therapy for chronic kidney disease: a meta-analysis. CJASN. 2012;7(3):391–400.

[11] Deb DK, Sun T, Wong KE, et al. Combined vitamin D analog and AT1 receptor antagonist synergistically block the development of kidney disease in a model of type 2 diabetes. Kidney Int. 2010;77(11):1000–1009.

[12] Fernandez-Juarez G, Luno J, Barrio V, et al. 25 (OH) vitamin D levels and renal disease progression in patients with type 2 diabetic nephropathy and blockade of the renin-angiotensin system. CJASN. 2013; 8(11):1870–1876.

[13] Zhang X, Song Z, Guo Y, et al. The novel role of TRPC6 in vitamin D ameliorating podocyte injury in STZ-induced diabetic rats. Mol Cell Biochem. 2015; 399(1-2):155–165.

[14] Wang B, Qian JY, Tang TT, et al. VDR/Atg3 axis regulates slit diaphragm to tight junction transition via

p62-mediated autophagy pathway in diabetic nephropathy. Diabetes. 2021.

[15] Li A, Yi B, Han H, et al. Vitamin D-VDR (vitamin D receptor) regulates defective autophagy in renal tubular epithelial cell in streptozotocin-induced diabetic mice via the AMPK pathway. Autophagy. 2021: 1–14.DOI:10.1080/15548627.2021.1962681

[16] Fujioka Y, Noda NN, Nakatogawa H, et al. Dimeric coiled-coil structure of Saccharomyces cerevisiae Atg16 and its functional significance in autophagy. J Biol Chem. 2010;285(2):1508–1515.

[17] Wu S, Zhang YG, Lu R, et al. Intestinal epithelial vitamin D receptor deletion leads to defective autophagy in colitis. Gut. 2015;64(7):1082–1094.

[18] Lu R, Zhang YG, Xia Y, et al. Imbalance of autophagy and apoptosis in intestinal epithelium lacking the vitamin D receptor. Faseb J. 2019;33(11):11845–11856.

[19] Song Z, Xiao C, Jia X, et al. Vitamin D/VDR protects against diabetic kidney disease by restoring podocytes autophagy. Diabetes Metab Syndr Obes. 2021;14:1681–1693.

[20] Gao W, Kang JH, Liao Y, et al. Biochemical isolation and characterization of the tubulovesicular LC3-positive autophagosomal compartment. J Biol Chem. 2010;285(2):1371–1383.

[21] Sun J. VDR/vitamin D receptor regulates autophagic activity through ATG16L1. Autophagy. 2016;12(6): 1057–1058.

[22] Haussler MR, Whitfield GK, Kaneko I, et al. Molecular mechanisms of vitamin D action. Calcif Tissue Int. 2013;92(2):77–98.

[23] Bikle DD. Vitamin D metabolism, mechanism of action, and clinical applications. Chem Biol. 2014;21(3): 319–329.

[24] Lee SM, Pike JW. The vitamin D receptor functions as a transcription regulator in the absence of 1,25-dihydroxyvitamin D3. J Steroid Biochem Mol Biol. 2016; 164:265–270.

[25] Yang Z, Klionsky DJ. Eaten alive: a history of macroautophagy. Nat Cell Biol. 2010;12(9):814–822.

[26] Livingston MJ, Ding HF, Huang S, et al. Persistent activation of autophagy in kidney tubular cells promotes renal interstitial fibrosis during unilateral ureteral obstruction. Autophagy. 2016;12(6):976–998.

[27] Lu R, Shang M, Zhang YG, et al. Lactic acid bacteria isolated from Korean kimchi activate the vitamin D receptor-autophagy signaling pathways. Inflamm Bowel Dis. 2020;26(8):1199–1211.